THE JOURNAL OF PHYSICAL CHEMISTRY Letters

Letter

pubs.acs.org/JPCL

# Contraction-Induced Changes in Hydrogen Bonding of Muscle Hydration Water

Hyok Yoo,[†] Ekaterina Nagornyak,[†] Ronnie Das,[†] Adam D. Wexler,[‡] and Gerald H. Pollack*[,†]

[†]Department of Bioengineering, University of Washington, Box 355061, Seattle, Washington 98195, United States

[‡]Wetsus Center for Sustainable Water Technology, Agora 1, 8900CC Leeuwarden, The Netherlands

Supporting Information

**ABSTRACT:** Protein−water interaction plays a crucial role in protein dynamics and hence function. To study the chemical environment of water and proteins with high spatial resolution, synchrotron radiation-Fourier transform infrared (SR-FTIR) spectromicroscopy was used to probe skeletal muscle myofibrils. Observing the OH stretch band showed that water inside of relaxed myofibrils is extensively hydrogen-bonded with little or no free OH. In higher-resolution measurements obtained with single isolated myofibrils, the water absorption peaks were relatively higher within the center region of the sarcomere compared to those in the I-band region, implying higher hydration capacity of thick filaments compared to the thin filaments. When specimens were activated, changes in the OH stretch band showed significant dehydrogen bonding of muscle water; this was indicated by increased absorption at ∼3480 $cm^{-1}$ compared to relaxed myofibrils. These contraction-induced changes in water were accompanied by splitting of the amide I (C═O) peak, implying that muscle proteins transition from $\alpha$-helix to $\beta$-sheet-rich structures. Hence, muscle contraction can be characterized by a loss of order in the muscle−protein complex, accompanied by a destructuring of hydration water. The findings shed fresh light on the molecular mechanism of muscle contraction and motor protein dynamics.

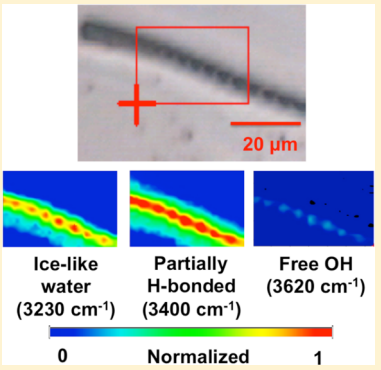


**SECTION:** Biophysical Chemistry and Biomolecules

While the importance of water for sustaining life is well-recognized, the exact role of water in biological processes remains unclear. On the other hand, an increasing number of studies show that biological processes are heavily influenced by interfacial water dynamics.[1]

One such water-mediated process is protein conformational change, which sits at the base of biological function.[2,3] X-ray crystallography studies had initially implied relatively few hydration layers adsorbed onto proteins, which could persist even under high vacuum.[4] However, recent experiments using THz and fluorescence spectroscopy have reveled that the dynamic hydration shells around proteins can extend out to much longer distances.[5,6] Further, recent dielectric spectroscopy studies have shown that protein folding is largely "slaved" by dynamics of water beyond the first several hydration layers,[7] that is, the protein follows the water.

The above-mentioned studies have sparked broad interest in hydration water. However, questions remain as to how such solution systems reflect the intricately ordered and crowded protein−water systems lying inside of intact tissues and cells. One such ordered system is muscle. When muscle is activated, proteins undergo synchronous conformational changes over millimeter and centimeter length scales. The protein changes are well studied; however, the changes in muscle water hydrogen bonding remain uncharted territory.

Many experimental observations imply that water may play an important role in muscle contraction (for a summary, see refs 8 and 9). Several recent findings in particular show that near-surface interfacial water is considerably more viscous than bulk water, with several groups reporting as high as 6-fold viscosity elevation near hydrophilic surfaces.[10] This high viscosity implies that the molecular cross-bridge swinging that has been considered central to the contractile process may experience resistance, and correspondingly, that the high energy needed to power such strokes might not be accounted for by ATP splitting alone.[11] This is but one of multiple issues raised by the presence of high-viscosity interfacial water.

Synchrotron radiation (SR) FTIR spectromicroscopy has lately emerged as a noninvasive probe of biological tissues with unprecedented spectral sensitivity and diffraction-limited spatial resolution, owing to its high brightness and small beam size.[12] This tool has proved especially useful in determination of chemical species and structures.[13−15] IR spectroscopy is also remarkably sensitive to the strength of hydrogen bonding as OH stretch frequency is linearly related to hydrogen bonding strength (i.e., stronger hydrogen bonding results in lower frequency of the OH stretching vibration).[16] With this technique, we examined possible changes of muscle water and protein structures associated with muscle contraction.

**Received:** January 14, 2014
**Accepted:** February 25, 2014
**Published:** February 25, 2014

  

In order to compare liquid water with muscle water, we first obtained the infrared spectrum of liquid water, as shown in Figure 1 (top). The OH stretch region of liquid water shows a broad peak due to extensive hydrogen bonding. The second derivative (below) shows that the broad peak resolves into three components, 3230, 3400, and 3620 $cm^{-1}$ corresponding, respectively, to the symmetric OH stretching mode of ice-like water, partially hydrogen-bonded water, and free OH. These are standard assignments. Of the three components, particularly notable is the one at 3400 $cm^{-1}$, which contains two shoulder peaks at 3480 and 3520 $cm^{-1}$. These shoulder peaks imply that liquid water may have at least three different arrangements of partially hydrogen-bonded water.

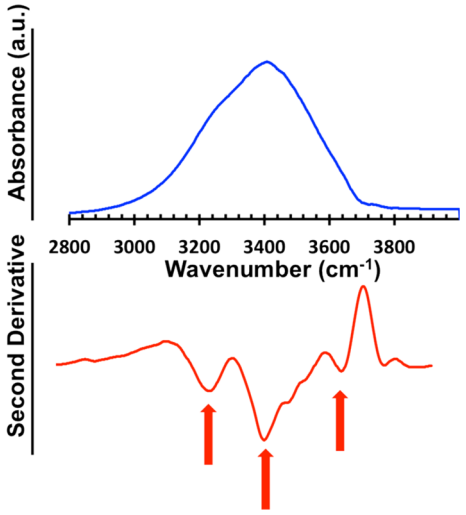


**Figure 1.** Infrared spectrum of liquid water at 22 °C in the OH stretch spectral region (top) and the second-derivative spectrum (bottom). Arrows indicate components resolved with second-derivative analysis at 3230, 3400, and 3620 $cm^{-1}$.

To observe the corresponding hydrogen bonding environment of muscle water, we collected an infrared map of a single relaxed honeybee myofibril (Figure 2). Panel (a) shows a bright-field image, with visible sarcomeres. The color images in panel (b) show absorption maps obtained at different spectral regions, corresponding to three components of liquid water determined above, fully coordinated ice-like water (3230 $cm^{-1}$), partially H-bonded water (3400 $cm^{-1}$), and free OH (3620 $cm^{-1}$). The strong relative absorptions at 3230 and 3400 $cm^{-1}$ indicate that the water inside of the relaxed myofibril is mostly "ice-like" and partially hydrogen-bonded. The weak absorption at 3620 $cm^{-1}$ indicates little or no free OH. Hence, most of the water molecules inside of the relaxed myofibril can be said to be either fully or partially hydrogen bonded.

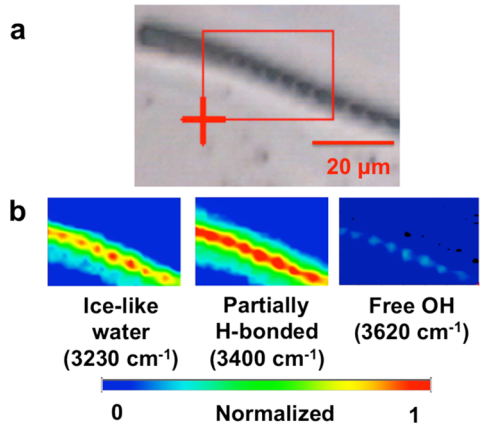


**Figure 2.** (a) Bright-field image of a single honeybee myofibril in the relaxed state. (b) IR absorption maps of the same specimen at three wavenumbers, corresponding to ice-like water (3230 $cm^{-1}$), partially hydrogen-bonded water (3400 $cm^{-1}$), and free OH (3620 $cm^{-1}$).

A particularly interesting feature of these infrared maps is the inhomogeneous spatial distribution of water along the myofibril. Overlaying the images showed that all three components of water IR absorption were higher in the center of the sarcomere than in the regions around the z-lines. Of those three components, the ice-like water was preferentially present in the middle of the sarcomere. The partially hydrogen-bonded water was spread more uniformly over the length of the myofibril, albeit slightly higher in the middle of the sarcomere. Thus, the water content within the myofibril shows sarcomeric periodicity. This may mean that the thick filaments, which are found in the middle of the sarcomere, might have higher water holding capacity than the thin filaments, which are nearer to the ends of the sarcomere. The stronger absorption of ice-like water may be due to higher negative charge density on the surfaces of thick filaments compared to that for thin filaments.[17,18]

In order to investigate the chemical changes associated with contraction, myofibril bundles were studied in relaxed and activated states. To simulate two physiological states of muscle, we used a standard model composed of skinned muscle and two physiological solutions. The bundle was first bathed in relaxing solution for 30 min, and an IR map was collected. Next, the same bundle was bathed in activating solution for 30 min. By that time, the specimen was fully contracted; all visible signs of contraction development had ceased.

Figure 3a shows bright-field images and superimposed IR maps of the relaxed and activated bundle. The IR maps were obtained at 3500 $cm^{-1}$, the spectral region showing the largest changes as the specimen passed from the relaxed state to the contracted state. The activated specimen absorbed significantly more than the relaxed specimen at 3500 $cm^{-1}$. This increase may be indicative of decreased hydrogen bonding strength of muscle water during contraction.

Figure 3b shows the representative IR spectra from relaxed (blue) and activated (red) specimens. Deionized water (green) is shown for comparison. Consistent with findings in the single myofibril (Figure 1), the spectra of the relaxed bundle show almost complete absence of free OH (3620 $cm^{-1}$) compared to liquid water. This indicates stronger hydrogen bonding strength of muscle water compared with that of deionized water. The most notable feature of Figure 3b is the shoulder peak near 3500 $cm^{-1}$ that appears upon activation, indicating "breakup" of the hydrogen bonding network. However, even with a significant dehydrogen bonding, the activated muscle still largely lacked free OH. The changes seen in the OH stretch region of IR spectra upon activation were reversible at least up to two activate−relax cycles, indicated by the appearance and disappearance of the a shoulder peak at 3500 $cm^{-1}$ in activated and relaxed states, respectively.

For more detailed spectral analysis of the OH stretch region, second-derivative analysis was performed on the original spectra. The results are shown in Figure 3c. They show several peaks corresponding to the symmetric and asymmetric $CH_2$


dx.doi.org/10.1021/jz5000879 | J. Phys. Chem. Lett. 2014, 5, 947−952

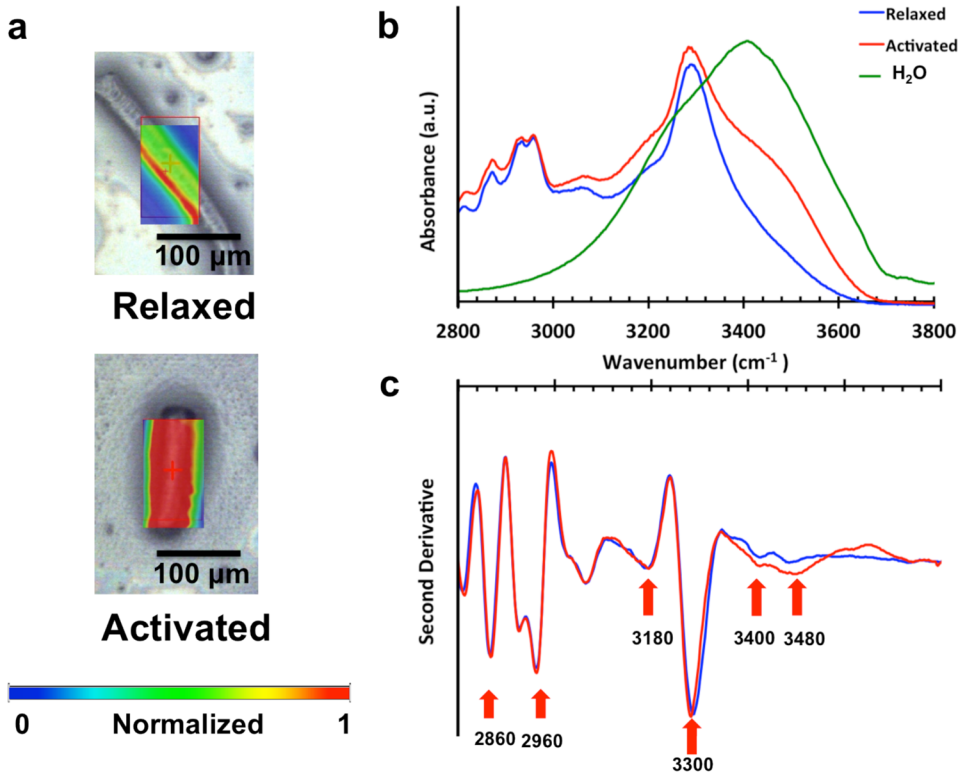


**Figure 3.** (a) Bright-field images of a relaxed and activated rabbit psoas myofibril bundle with overlays of IR images at 3500 $cm^{-1}$ showing a significant increase in absorption during contraction. For the color map, the absorption of activated muscle at 3550 $cm^{-1}$ is normalized to 1 for comparison. (b) IR spectra of relaxed (blue) and activated (red) muscle and deionized water (green). (c) Second-derivative spectra of relaxed and activated muscle.

stretches of the lipids (~2852 and 2924 $cm^{-1}$), the asymmetric $CH_3$ stretch of the lipids (2960 $cm^{-1}$), the symmetric NH stretch of amide A and amide B (3300 and 3057 $cm^{-1}$), besides the water peaks (3180, 3400, 3480 $cm^{-1}$). Table 1 summarizes

**Table 1. Assignment of IR Bands and Their Major Contributors**

| wavenumber ($cm^{-1}$) | vibrational mode assignment and major contribution |
|---|---|
| ~3620 | $\nu$OH of free OH[19] |
| ~3400 | $\nu$OH of partially hydrogen-bonded water19 |
| ~3300 | amide A, $\nu$NH of proteins[20] |
| ~3230 | $\nu$OH of ice-like water[19] |
| ~2960 | $\nu_{as}CH_3$ of lipids, proteins and nucleic acids[20] |
| ~2924 | $\nu_{as}CH_2$ of lipids[21] |
| ~2860 | $\nu_{s}CH_2$ of lipids[21] |
| ~1650 | amide I, $\nu$C=O stretch[20] |
| ~1550 | amide II[20] |

those peaks. While other peaks do not show any obvious shifts, the amide A band shows a blue shift (i.e., to higher frequency) of about 10 $cm^{-1}$. Such a shift has been associated with an $\alpha$-helix to $\beta$-sheet transition.[16]

In Figure 3c, second-derivative water peaks are seen corresponding to 3180, 3400, and 3480 $cm^1$. Compared with liquid water (Figure 1), the component corresponding to ice-like water occurs at a lower frequency, by about 20 $cm^{-1}$. This shift indicates that fully coordinated modes of water in muscle contain slower vibrational modes, presumably due to dipolar coupling of water and protein oscillators. Upon activation, the ratio of the amide A peak (3300 $cm^{-1}$) and the 3480 $cm^{-1}$ water peak increases, showing an increase in the number of broken hydrogen bonds per protein molecule. Thus, the second-derivative analysis confirms the results obtained from the original spectra, a significant breakup of hydrogen bonds during activation. The absence of free OH in both relaxed and activated myofibril bundles shows that the breakup of hydrogen bonding during activation still leaves water molecules hydrogen-bonded to at least one neighboring water molecule.

To confirm that the observed changes in muscle water are not artifacts arising from differences in absorption from the different physiological solutions, we collected infrared spectra of both activating and relaxing solutions (Figure S1, Supporting Information). Comparison with the spectra of deionized water confirmed that both physiological solutions had IR spectra indistinguishable from that of deionized water.

The amide bands in vibrational spectra of proteins are useful tools for determining the secondary structure of proteins and the proteins' stability.[22] Specifically, the amide I peak provides sensitive information on protein secondary structures (i.e., $\alpha$-helix, $\beta$-sheets, $\beta$-sheet turns, side chains, etc.).[23] Figure 4a shows representative spectra of the corresponding spectral region in relaxed (blue) and activated (red) myofibril bundles. These spectra were taken from the same spectra as Figure3b. In the relaxed state, the myofibril bundle shows a classic amide I peak centered at ~1650 $cm^{-1}$ and an amide II peak centered at ~1550 $cm^{-1}$. Upon activation, the amide I peak splits into two (Figure 4a), the new peak appearing at ~1600 $cm^{-1}$, over and above the original peak at ~1650 $cm^{-1}$. Moreover, the centroid of the 1650 $cm^{-1}$ peak is red-shifted to lower frequency by about 15 $cm^{-1}$. While detailed theoretical description of amide I splitting has posed significant challenges, experimental results


dx.doi.org/10.1021/jz5000879 | J. Phys. Chem. Lett. 2014, 5, 947−952

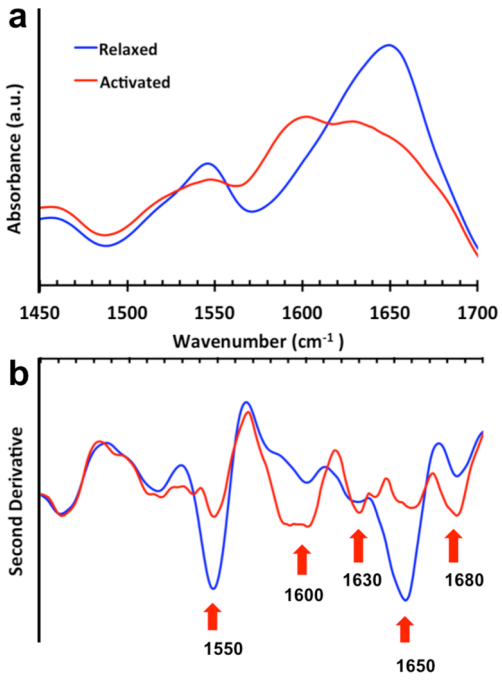


**Figure 4.** (a) IR spectra of a relaxed (blue) and activated (red) myofibril bundle in amide I and II spectral regions. (b) Second derivative of the IR spectra.

indicate that splitting of the amide I peak to lower frequency is associated with $\beta$-sheet-rich structures.[24] Thus, the red shifting of the 1650 $cm^{-1}$ peak centroid indicates the formation of intermolecular $\beta$-sheets arising out of aggregation of unfolded proteins in activated muscle. The new peak appearing in the amide I region at ~1600 $cm^{-1}$ is assigned to the amino acid side chains of proteins including both hydrogenated and hydroxylated glutamine (H-Gly and OH-Gly), whose transport plays an important role in phosphorylation of muscle and contraction.[20,25] Thus, increased absorption at ~1600 $cm^{-1}$ seen here may be due to formation of side chains during contraction. Contrary to the amide I band, the amide II band showed less change with activation: diminished absorbance, with no change in the peak location.

To examine these spectral features in more detail, we looked at the second-derivative spectra. Figure 4b shows the second derivative of the original spectra in the amide I and II region. Several features are of interest. First, the relaxed muscle has markedly higher composition of $\alpha$-helix (1652 $cm^{-1}$) than activated muscle. Second, the peaks centered at ~1630 and ~1680 $cm^{-1}$ increased significantly in amplitude when muscle went from relaxed to activated. These peaks represent $\beta$-sheets and $\beta$-turns, respectively.[20] Taken together, these findings show that muscle proteins lost helical order during activation, similar to the conclusions drawn earlier from X-ray diffraction studies.[26]

The activation-associated changes of muscle water are appreciable (Figure 2b). However, the myofibril bundle contains water both inside of the myofibril and between the myofibrils. To ensure that the observed changes in hydrogen bonding are indeed due to changes within the myofibrils, that is, associated with myosin, actin, and so forth, we probed single myofibrils, where the only water present in the sample lies within the contractile apparatus. Contraction is ordinarily less pronounced in honeybee myofibrils but was confirmed by monitoring shortening of sarcomeres in bright-field images. The statistics are summarized in Figure S2 (Supporting Information).

The results obtained with the single myofibril (Figure 5) largely concur with those obtained with the myofibril bundles

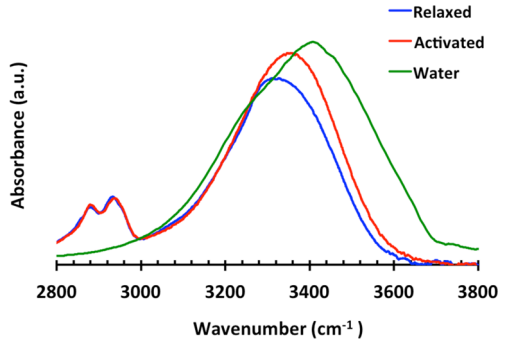


**Figure 5.** IR spectra of a relaxed (blue) and activated single myofibril (red). The IR spectrum of liquid water is shown for comparison (green).

(Figure 4). As seen with rabbit myofibril bundles (Figure 3b), the representative spectrum of relaxed single myofibril shows an OH stretch peak significantly red-shifted from that of deionized water. This shift indicates stronger hydrogen bonding than liquid water. Moreover, as the specimen passed from relaxed (blue) to activated (red), the hydrogen bonding strength decreased, as indicated by a ~25 $cm^{-1}$ blue shifting of the centroid of the water OH stretch peak. The dehydrogen bonding agrees with results obtained from myofibril bundles. Hence, the major findings in muscle water hydrogen bonding are consistent in both single myofibrils and myofibril bundles, indicating that those changes occur within the actomyosin complex.

This study was carried out to understand the chemical environment of skeletal muscle water and its possible role in contraction. Our results show that water in relaxed muscle is significantly more structured than bulk water, with little or no free OH present. This was found inside of myofibril bundles as well as inside of single myofibrils. The most notable result of this study was the sensitivity of the water hydrogen bonding environment to distinct physiological states. When the myofibril was activated, the well-hydrogen-bonded muscle water lost order as the muscle proteins changed conformation. Water evidently plays some role in the contractile process.

It is widely believed that water inside of biological tissues is similar to bulk water, except for the first two or three protein hydration layers. However, more recent results have shown that hydrophilic surfaces can extensively order nearby water.[27−29] Further, recent NMR measurements show that in confined geometries such as inside of reverse micelles, protein hydration shells can extend out to several dozens of layers.[30] Considering the confined geometry inside of the myofilament lattice, it is no surprise that most of the muscle water is well-structured. Thus, muscle water differs substantially from bulk water.

While modern understanding of muscle contraction is largely dominated by the cross-bridge theory originally proposed by Sir Andrew Huxley and H. E. Huxley,[31,32] many experimental results remain at odds with that theory. The most notable are shortening of thick filaments during contraction[33] and generation of force even with no apparent overlap of thick and thin filaments,[34] where no attachment of myosin heads to actin filaments can occur. Both findings indicate the need for


dx.doi.org/10.1021/jz5000879 | J. Phys. Chem. Lett. 2014, 5, 947−952

reconsideration of that mechanism.[9,35] On the other hand, the breakup of water structure during contraction implies that the high viscosity issue mentioned above may be less of a problem for the prevailing theory than initially considered. If the water remained highly viscous, not only could cross-bridges fail to swing, but also, any kind of filamentary motion might confront substantial difficulty.

Several physical changes occur immediately following stimulation but prior to force generation. These include changes in thick filament length,[33] sudden decreases in viscoelasticity,[36] loss of axial and helical order in myosin,[37] and latency relaxation.[38] All of those changes occur within milliseconds after stimulation and well before the onset of force generation. While these changes are seemingly necessary preconditions for force generation, their mechanisms have remained unclear. Changes in water structure might potentially explain some or all of those changes and help provide better understanding of the molecular mechanism of muscle contraction.

Given the breakup of water structure during contraction, a lingering question is which of the two events comes first, changes in protein conformation or breakup of ordered hydration water. Time-resolved studies will be needed to answer this important question, which may have relevance also for other biological systems.

## METHODS

*Solutions.* Several different solutions were used to simulate different states of contraction. Relaxing solution (pH 7.0) had a composition (in mM) of 10 MOPS, 64.4 $K^+$ propionate, 5.23 $Mg^{2+}$ propionate, 9.45 $Na_2SO_4$, 10 EGTA, 0.188 $CaCl_2$, 7 ATP, and 10 creatine phosphate. Activating solution consisted (in mM) of 10 MOPS, 45.1 $K^+$ propionate, 5.21 $Mg^{2+}$ propionate, 9.27 $Na_2SO_4$, 10 EGTA, 9.91 $CaCl_2$, 7.18 ATP, and 10 creatine phosphate. Glycerol solution consisted of half glycerol and half rigor solution, the latter containing (in mM) 50 Tris (pH 7.4), 100 NaCl, 2 KCl, 2 $MgCl_2$, and 10 EGTA.

*Skeletal Myofibril Preparation.* Two types of specimens were studied, myofibril bundles and single myofibrils. Myofibril bundles were prepared from rabbit psoas muscles. Briefly, muscles were dissected bluntly from the backs of rabbits, along the length of the fibers. They were cut into thin strips and tied at both ends to a wooden stick in order to maintain their natural length. The prepared muscle strips were placed in glycerol solution and stored in a freezer at −20 °C for long-term storage. To obtain myofibril bundles, the muscle strips stored in glycerol solution were transferred to rigor solution for 60 min and then cut into 2 mm segments across the fiber cross section. A tissue segment was diced using a blender (Sorvall Omni Mixer) in 7 mL of rigor solution using the following protocol: twice × 5 s at 1100 rpm, once × 5 s at 2500 rpm, and once × 1 s at 3100 rpm. The resulting myofibril bundles were typically about 50 μm in diameter and several hundred micrometers long. Eight myofibril bundles were probed both in relaxed and activated states to confirm the consistency of the data ($n$ = 8).

Single honeybee myofibrils were prepared from the thorax region of honeybee flight muscles. The dissected specimen was stored at −20 °C in a 50/50 glycerol/rigor solution mixture for long-term storage. To prepare single myofibrils, the muscle tissue was washed in rigor solution and cut using a blender in 2 mL of rigor solution using the following protocol: once × 5 s at 2500 rpm and once × 10 s at 4000 rpm. The resulting myofibrils were typically 4−5 μm in diameter and tens of micrometers long. Ten single myofibril samples were probed in both activated and relaxed states for consistency ($n$ = 10).

*Synchrotron Radiation Fourier Transform Infrared (SR-FTIR) Spectromicroscopy.* The SR-FTIR measurements were made using a Nicolet Magna 760 FTIR bench and a Nicolet Nic-Plan IR microscope with 15× and 32× objectives, at the Advanced Light Source, Lawrence Berkeley National Laboratory, Infrared Beamline 1.4.3. Myofibril bundle experiments were carried out with a 15× objective, while single myofibril experiments were carried out using a 32× objective. Thirty-two scans of IR spectra were collected between 800 and 4000 $cm^{-1}$ at 4 $cm^{-1}$ resolution and averaged. SR-FTIR spectra were initially collected to identify the chemical environment of relaxed muscle. To do this, a drop of myofibril bundle suspension was dispensed onto a $CaF_2$ window and then immersed in relaxing solution for 30 min on ice. To collect the SR-FTIR spectra of activated muscle, activating solution was drop dispensed onto the myofibril bundle, and measurements were made after the specimen had visibly finished contracting. For obtaining spectral maps of myofibril bundles, a total of eight myofibril bundles were probed in both relaxed and activated states for consistency. Each sample was scanned with a 5 μm step size. For single honeybee myofibrils, 13 myofibrils were probed in both relaxed and activated states. Each sample was scanned with a 1 μm step size. Second-derivative analysis was performed for enhancement of spectral resolution using the Savitsky−Golay method.[39] To minimize evaporation during data collection, the myofibril bundle was kept in a water-tight custom chamber with a Tefon fitting.

## ASSOCIATED CONTENT

### Supporting Information

Description of the material included along with IR spectra. This material is available free of charge via the Internet at http://pubs.acs.org.

## AUTHOR INFORMATION

### Corresponding Author

*E-mail: ghp@u.washington.edu

### Notes

The authors declare no competing financial interest.

## ACKNOWLEDGMENTS

This study was supported by a grant from the NIH (5R01 GM093842). The Advanced Light Source is supported by the Director, Office of Science, Office of Basic Energy Sciences, of the U.S. Department of Energy under Contract No. DE-AC02-05CH11231.

## REFERENCES

(1) Chaplin, M. Do We Underestimate the Importance of Water in Cell Biology? *Nat Rev Mol Cell Biol* **2006**, *7*, 861−866.

(2) Cheung, M. S.; Garcia, A. E.; Onuchic, J. N. Protein Folding Mediated by Solvation: Water Expulsion and Formation of the Hydrophobic Core Occur after the Structural Collapse. *Proc. Natl. Acad. Sci. U.S.A.* **2002**, *99*, 685−690.

(3) Makarov, V.; Pettitt, B. M.; Feig, M. Solvation and Hydration of Proteins and Nucleic Acids: A Theoretical View of Simulation and Experiment. *Acc. Chem. Res.* **2002**, *35*, 376−384.

(4) Svergun, D. I.; Richard, S.; Koch, M. H. J.; Sayers, Z.; Kuprin, S.; Zaccai, G. Protein Hydration in Solution: Experimental Observation

by X-ray and Neutron Scattering. *Proc. Natl. Acad. Sci. U.S.A.* **1998**, *95*, 2267−2272.
(5) Born, B.; Kim, S. J.; Ebbinghaus, S.; Gruebele, M.; Havenith, M. The Terahertz Dance of Water with the Proteins: The Effect of Protein Flexibility on the Dynamical Hydration Shell of Ubiquitin. *Faraday Discuss.* **2009**, *141*, 161−173.
(6) Ebbinghaus, S.; Kim, S. J.; Heyden, M.; Yu, X.; Heugen, U.; Gruebele, M.; Leitner, D. M.; Havenith, M. An Extended Dynamical Hydration Shell around Proteins. *Proc. Natl. Acad. Sci. U.S.A.* **2007**, *104*, 20749−20752.
(7) Frauenfelder, H.; Chen, G.; Berendzen, J.; Fenimore, P. W.; Jansson, H.; McMahon, B. H.; Stroe, I. R.; Swenson, J.; Young, R. D. A Unified Model of Protein Dynamics. *Proc. Natl. Acad. Sci. U.S.A.* **2009**, *106*, 5129−5134.
(8) Oplatka, A. Critical Review of the Swinging Crossbridge Theory and of the Cardinal Active Role of Water in Muscle Contraction. *Crit. Rev. Biochem. Mol. Biol.* **1997**, *32*, 307−360.
(9) Pollack, G. H. *Muscles & Molecules: Uncovering the Principles of Biological Motion*; Ebner & Sons Publishers: Seattle, WA, 1990; p 300.
(10) Goertz, M. P.; Houston, J. E.; Zhu, X. Y. Hydrophilicity and the Viscosity of Interfacial Water. *Langmuir* **2007**, *23*, 5491−5497.
(11) Widdas, W. F.; Baker, G. F. The Surface Energy of Water: The Largest but Forgotten Source of Energy in Biological Systems. *Cytobios* **2001**, *106*, 7−54.
(12) Levenson, E.; Lerch, P.; Martin, M. C. Spatial Resolution Limits for Synchrotron-Based Infrared Spectromicroscopy. *Infrared Phys. Technol.* **2008**, *51*, 413−416.
(13) Holman, H.-Y. N.; Bechtel, H. A.; Hao, Z.; Martin, M. C. Synchrotron IR Spectromicroscopy: Chemistry of Living Cells. *Anal. Chem.* **2010**, *82*, 8757−8765.
(14) Holman, H.-Y. N.; Hao, Z.; Martin, M. C.; Bechtel, H. A. Infrared Spectromicroscopy: Probing Live Cellular Responses to Environmental Changes. *Synchrotron Radiat. News* **2010**, *23*, 12−19.
(15) Holman, H.-Y. N.; Miles, R.; Hao, Z.; Wozei, E.; Anderson, L. M.; Yang, H. Real-Time Chemical Imaging of Bacterial Activity in Biofilms Using Open-Channel Microfluidics and Synchrotron FTIR Spectromicroscopy. *Anal. Chem.* **2009**, *81*, 8564−8570.
(16) Falk, M.; Ford, T. A. Infrared Spectrum and Structure of Liquid Water. *Can. J. Chem.* **1966**, *44*, 1699−1707.
(17) Noble, M. I.; Pollack, G. H. Molecular Mechanisms of Contraction. *Circ. Res.* **1977**, *40*, 333−342.
(18) Yu, L. C.; Dowben, R. M.; Kornacker, K. The Molecular Mechanism of Force Generation in Striated Muscle. *Proc. Natl. Acad. Sci. U.S.A.* **1970**, *66*, 1199−1205.
(19) Falk, M.; Ford, T. A. Infrared Spectrum and Structure of Liquid Water. *Can. J. Chem.* **1966**, *44*, 1699−.
(20) Barth, A. Infrared Spectroscopy of Proteins. *Biochim. Biophys. Acta* **2007**, *1767*, 1073−1101.
(21) Birarda, G.; Grenci, G.; Businaro, L.; Marmiroli, B.; Pacor, S.; Piccirilli, F.; Vaccari, L. Infrared Microspectroscopy of Biochemical Response of Living Cells in Microfabricated Devices. *Vib. Spectrosc.* **2010**, *53*, 6−11.
(22) Byler, D. M.; Susi, H. Examination of the Secondary Structure of Proteins by Deconvolved FTIR Spectra. *Biopolymers* **1986**, *25*, 469−487.
(23) Pelton, J. T.; McLean, L. R. Spectroscopic Methods for Analysis of Protein Secondary Structure. *Anal. Biochem.* **2000**, *277*, 167−176.
(24) Litvinov, R. I.; Faizullin, D. A.; Zuev, Y. F.; Weisel, J. W. The $\alpha$-Helix to $\beta$-Sheet Transition in Stretched and Compressed Hydrated Fibrin Clots. *Biophys. J.* **2012**, *103*, 1020−1027.
(25) Rennie, M. J.; Low, S. Y.; Taylor, P. M.; Khogali, S. E.; Yao, P. C.; Ahmed, A. Amino Acid Transport During Muscle Contraction and Its Relevance to Exercise. *Adv. Exptl. Med. Biol.* **1998**, *441*, 299−305.
(26) Reconditi, M.; Brunello, E.; Linari, M.; Bianco, P.; Narayanan, T.; Panine, P.; Piazzesi, G.; Lombardi, V.; Irving, M. Motion of Myosin Head Domains during Activation and Force Development in Skeletal Muscle. *Proc. Natl. Acad. Sci. U.S.A.* **2011**, *108*, 7236−7240.
(27) Yoo, H.; Paranji, R.; Pollack, G. H. Impact of Hydrophilic Surfaces on Interfacial Water Dynamics Probed with NMR Spectroscopy. *J. Phys. Chem. Lett.* **2011**, *2*, 532−536.
(28) Zheng, J.-m.; Pollack, G. H. Long-Range Forces Extending from Polymer−Gel Surfaces. *Phys. Rev. E* **2003**, *68*, 031408.
(29) Pollack, G. H. *The Fourth Phase of Water: Beyond Solid, Liquid, and Vapor*; Ebner and Sons: Seattle, WA, 2013.
(30) Nucci, N. V.; Pometun, M. S.; Wand, A. J. Site-Resolved Measurement of Water−Protein Interactions by Solution NMR. *Nat. Struct. Mol. Biol.* **2011**, *18*, 245−249.
(31) Huxley, H.; Hanson, J. Changes in the Cross-Striations of Muscle During Contraction and Stretch and Their Structural Interpretation. *Nature* **1954**, *173*, 973−976.
(32) Huxley, A. F. Muscle Structure and Theories of Contraction. *Prog. Biophys. Biophys. Chem.* **1957**, *7*, 255−318.
(33) Nagornyak, E. M.; Blyakhman, F. A.; Pollack, G. H. Stepwise Length Changes in Single Invertebrate Thick Filaments. *Biophys. J.* **2005**, *89*, 3269−3276.
(34) Carlsen, F.; Knappeis, G. G.; Buchthal, F. Ultrastructure of the Resting and Contracted Striated Muscle Fiber at Different Degrees of Stretch. *J. Biophys. Biochem. Cytol.* **1961**, *11*, 95−117.
(35) Pollack, G. H. *Cells, Gels and the Engines of Life: A New, Unifying Approach to Cell Function*; Ebner & Sons: Seattle, WA, 2001; p 305.
(36) Ford, L. E.; Huxley, A. F.; Simmons, R. M. Tension Responses to Sudden Length Change in Stimulated Frog Muscle Fibres near Slack Length. *J. Physiol.* **1977**, *269*, 441−515.
(37) Brunello, E.; Bianco, P.; Piazzesi, G.; Linari, M.; Reconditi, M.; Panine, P.; Narayanan, T.; Helsby, W. I.; Irving, M.; Lombardi, V. Structural Changes in the Myosin Filament and Cross-Bridges during Active Force Development in Single Intact Frog Muscle Fibres: Stiffness and X-ray Diffraction Measurements. *J. Physiol.* **2006**, *577*, 971−984.
(38) Lännergren, J. The Effect of Low-Level Activation on the Mechanical Properties of Isolated Frog Muscle Fibers. *J. Gen. Physiol.* **1971**, *58*, 145−162.
(39) Savitzky, A.; Golay, M. J. E. Smoothing and Differentiation of Data by Simplified Least Squares Procedures. *Anal. Chem.* **1964**, *36*, 1627−1639.